

Reductive Deposition of Cu on Porous Silicon from Aqueous Solutions: An X-ray Absorption Study at the Cu L_{3,2} Edge

T. K. Sham,^{*,†} I. Coulthard,[†] J. W. Lorimer,[†] A. Hiraya,[‡] and M. Watanabe[‡]

Department of Chemistry, The University of Western Ontario, London, N6A 3B7 Canada, and UVSOR, Institute for Molecular Science, Okazaki, 44 Japan

Received May 11, 1994. Revised Manuscript Received July 25, 1994[⊗]

The reductive deposition of metallic Cu on porous silicon (PS) surface from aqueous solution of Cu²⁺(aq) ions is reported. X-ray absorption near-edge structure (XANES) at the Cu L_{3,2} edge has been used to characterize these samples. It is found that the reduction of Cu²⁺(aq) to Cu occurs readily at room temperature and appears to be controlled by the availability of active sites as well as the concentration of Cu²⁺(aq) and that only a very thin film of Cu is formed even with concentrated solutions. The surface of Cu/PS is oxidized when exposed to the ambient atmosphere. The spectroscopic features and the implication of the results are discussed.

Introduction

The recent discovery of photoluminescence from porous silicon (PS) at room temperature has generated a great deal of interest in semiconductor materials research.^{1,2} This is partly because intense luminescence in the visible from silicon at room temperature is a new phenomenon and partly because of the implications of the availability of a silicon light emitter for new electronic and optoelectronic technology.

Porous silicon is crystalline silicon with pillar and nodule structures of nanometer size.^{3–5} It can be produced easily by electrochemical etching of Si wafers in HF solutions. Porous silicon was first prepared in the 1950s⁶ but it received little attention until 1990 when room-temperature luminescence was reported.¹ Since then there have been extensive studies of porous silicon in both basic and applied materials research.⁷ It now appears that the most viable explanation for the origin of luminescence by porous silicon is the quantum confinement model:^{1,3,4,8,9} electrons and holes confined in the nanostructure are responsible for the luminescence, although under some circumstances surface species may also contribute.^{10,11} The objective of this paper,

however, is to report a recent investigation on another relatively unexplored aspect of porous silicon research, the chemistry of its vast internal surface, and its implication for catalysis.^{12,13}

Porous silicon prepared electrochemically in a HF–ethanol solution from a Si wafer such as a Si(100) single crystal has typically a thickness of a few microns to tens of microns and an internal surface area of 200–1000 m²/cm³ depending on the porosity.^{8–10} These values are comparable to the surface area of silica and alumina supports used in industrial catalysts.¹³ Thus it appears that porous silicon itself, with its high hydrogen content, may exhibit catalytic activity toward hydrogenation reactions and that the large internal surface may act as a support for metal catalysts. The latter is the main concern here. Two recent reports^{12,14} already showed that porous silicon is an excellent reducing agent toward the reduction of Cu and noble-metal ions from aqueous solution.

In this paper, we report details of the preparation and characterization of Cu deposited on porous silicon from aqueous solutions. Using high-resolution X-ray absorption near-edge structure (XANES) spectroscopy we have examined the Cu L_{3,2} edge XANES of the Cu deposited reductively on porous silicon surface from Cu²⁺(aq) in aqueous solution using both the total electron yield (TEY) and fluorescence (FLY) detection schemes. The TEY technique is more surface sensitive than FLY which is essentially a bulk sensitive technique when a bulk sample is measured. Thus, we can reveal some details about the nature of Cu on the PS surface by making simultaneous measurements with both these techniques, where the sampling depth is determined by

* To whom correspondence should be addressed.

† The University of Western Ontario.

‡ UVSOR, Institute of Molecular Science.

⊗ Abstract published in *Advance ACS Abstracts*, September 15, 1994.

- (1) Canham, L. T. *Appl. Phys. Lett.* **1990**, *57*, 1046.
- (2) Sailor, M. J.; Kavanagh, K. L. *Adv. Mater.* **1992**, *4*, 432.
- (3) Cullis, A. G.; Canham, L. T. *Nature* **1991**, *353*, 335.
- (4) Lehmann, V.; Gösele, U. *Appl. Phys. Lett.* **1990**, *58*, 856.
- (5) Sham, T. K.; Feng, X. H.; Jiang, D. T.; Yang, B. X.; Xiong, J. Z.; Bzowski, A.; Houghton, D. C.; Bryskiewicz, B.; Wang, E. *Can. J. Phys.* **1992**, *70*, 813.
- (6) Uhlir, A. *Bell. Syst. Tech. J.* **1956**, *35*, 333. Turner, D. R. *J. Electrochem. Soc.* **1958**, *105*, 402.
- (7) Sham, T. K.; Jiang, D. T.; Coulthard, I.; Lorimer, J. W.; Feng, X. H.; Tan, K. H.; Frigo, S. P.; Rosenberg, R. A.; Houghton, D. C.; Bryskiewicz, B. *Mater. Res. Soc. Symp. Proc.* **1992**, *281*, 525.
- (8) Herino, R.; Billat, S.; Bsiesy, F.; Gaspard, M.; Mihalesca, I.; Ramestain, R.; Vial, J. C. *Phys. Scr.* **1992**, *T45*, 300.
- (9) Sham, T. K.; Jiang, D. T.; Coulthard, I.; Lorimer, J. W.; Feng, X. H.; Tan, K. H.; Frigo, S. P.; Rosenberg, R. A.; Houghton, D. C.; Bryskiewicz, B. *Nature* **1993**, *363*, 331.
- (10) Jiang, D. T.; Coulthard, I.; Sham, T. K.; Lorimer, J. W.; Frigo, S. P.; Feng, X. H.; Rosenberg, R. A. *J. Appl. Phys.* **1993**, *74*, 6335.

(11) Deak, P.; Rosenbauer, M.; Stutzmann, M.; Weber, J.; Brandt, M. S. *Phys. Rev. Lett.* **1992**, *69*, 2531.

(12) Coulthard, I.; Jiang, D. T.; Lorimer, J. W.; Sham, T. K.; Feng, X. H. *Langmuir* **1993**, *9*, 3441.

(13) Moss, R. L. *Aspects of the Characterization and Activity of Supported Metal and Bimetallic Catalysts; Special Periodic Report, Catalysis* **1981**, *4*, 31.

(14) Anndsgager, D.; Hilliard, J.; Hetrick, J.; Abuhassan, L. H.; Plisch, M.; Nayfeh, M. H.; J. Appl. Phys. **1993**, *74*, 4783. Coulthard, I.; Lorimer, J. W.; Sham, T. K. *Abstract 824RNP, 118th Mtg. Electrochem. Soc., Toronto, Oct 1992.*

the electron escape depth (1 nm in this case)¹⁵ in TEY and the Cu L-edge fluorescent X-ray attenuation length (>100 nm)¹⁶ in FLY. This paper is organized as follows: In the section below, the chemical properties of porous silicon relevant to the reductive deposition of Cu from aqueous solutions are described briefly, and then a description of X-ray absorption spectroscopy and its application in the context of this work is given. Experimental procedures are presented next, followed by results, discussion, and conclusions.

Chemical Properties of Porous Silicon

Porous silicon is a network of interconnecting crystalline silicon structures with dimensions of nanometres. It can also be viewed as a silicon sponge with porosity as high as 65–85%⁸ and consequently a large internal volume of unoccupied space of comparable dimension and a vast internal surface area. Thus the chemistry of the internal surface plays a crucial role in the chemical properties of porous silicon. The internal surface of an as-prepared porous silicon layer (typically micrometers thick on a Si wafer substrate) from a HF solution is usually passivated by hydrogen.¹⁷ After exposure to ambient atmosphere and rinsing with distilled water, the surface becomes oxidized forming native silicon oxide which undergoes hydrolysis leading to possible acidic and basic –Si–OH sites on the surface.¹⁸ We have used four chemical tests to characterize the chemical properties of PS.¹⁴ These are (a) reaction with water, (b) reaction with strong base, (c) reaction with strong acid, and (d) reaction with metal ions, either aquo or complex, in aqueous solution.

With water, we found that PS dissolves slowly with very slow evolution of H₂; the entire PS layer disappears overnight leaving behind a smooth Si substrate. With strong aqueous metal hydroxides, we found that PS reacts vigorously to produce hydrogen gas and the PS layer is destroyed. This observation differs somewhat from, but is not inconsistent with, another report of the removal of the surface oxide with aqueous NaOH under milder conditions.¹⁹ With concentrated HNO₃, the reaction is explosive and produces a light flash as well as NO₂, in agreement with another report.¹⁹ These observations indicate that PS is a good reducing agent. With metal ions, we found that Cu(II) aquo ions as well as a number of noble metal ions in aqueous solutions are reduced readily by porous silicon. More importantly, PS seems to be able to reduce ions for which the reduction potential is positive.^{12,14} In addition to these tests, aging in the ambient environment passivates the PS surface and produces more intense luminescence with shorter wavelengths. This behavior is similar to those reported in the literature for the electrooxidized porous silicon.⁸

(15) Electrons primarily responsible for the TEY are the Cu LVV Auger (<900 eV), and secondary electrons (energy distribution maximum ~15 eV). These electrons would have an escape depth of the order of 1 nm according to the universal curve of attenuation length of electron in solids. For details see: Erbil, A.; Cargill III, G. S.; Frahm, R.; Boehme, R. F. *Phys. Rev. B*, **1988**, *37*, 2450.

(16) The total absorption coefficient of Cu at the Cu L fluorescent X-ray energy (~930 eV) is 1.59×10^3 cm²/g according to Henke et al. *At. Dat. Nucl. Dat. Tables* **1982**, *27*, 1. The corresponding 1/e attenuation length of the soft X-rays by Cu is 700 nm.

(17) This is a well-known fact, and we have reflectance IR and synchrotron results to show that this is indeed the case in our samples.

(18) *Faraday Soc. Discuss.* **1971**, No. 52, *Surface Chemistry of Oxides*.

(19) McCord, P.; Yau, S.-L.; Bard, A. J. *Science* **1992**, *257*, 68.

X-ray Absorption Near-Edge Structure (XANES)

XANES refers to the spectral features in approximately the first 50 eV of the X-ray absorption coefficients above an absorption edge (threshold for the photoexcitation of a core electron).^{20,21} It arises from dipole transitions ($\Delta l = 1$, $\Delta j = 0, \pm 1$) from the atomic core to previously unoccupied molecular orbitals (bound states) and quasi-bound (multiple scattering resonance) states in the vicinity of the vacuum level. XANES often exhibits a spike at the threshold called whiteline (sharp and intense whitelines are seen in materials with high and localized unoccupied densities of states in the vicinity of the Fermi level in metals and low-lying unoccupied molecular orbitals in molecules) followed by some less intense resonance features at higher photon energies characteristic of the local structure (first three shells of neighboring atoms surrounding the absorbing atom).^{20,21} In the case of metals which exhibit long-range order, the XANES feature is characteristic of the band structure of the metal. Metal clusters usually exhibit qualitatively similar XANES features with less pronounced resonances. The XANES of metal clusters and multilayers approaches that of the metal XANES as the cluster size and layer thickness increases.²⁰ Typically, three to four layers are required to produce the gross feature of a bulk metal spectrum.

Cu L_{3,2} edge XANES refers to the near-edge photoexcitation spectrum of the Cu 2p_{3/2} and 2p_{1/2} levels, respectively. The dipole selection rule dictates that the Cu 2p_{3/2} level probes the unoccupied state of Cu 3d_{5/2} and 3d_{3/2} character while Cu 2p_{1/2} probes the Cu 3d_{3/2} character. (The p to s transition, which is also dipole allowed, is significantly less intense than that of the $\Delta l = +1$, p-d transition due to matrix element and densities of states effects.) A strong whiteline at the Cu L_{2,3} edge indicates that there exist localized unoccupied 3d states just above the Fermi level and the area under the curve of the whiteline is correlated with the unoccupied densities of states (d hole counts) at the Cu site.^{22–24} These L-edge features have often been used to study the role of d electron distribution in chemical trends in materials containing 3d,^{25–27} 4d,^{28–30} and 5d^{31–34} metals. Thus by comparing the XANES of Cu/PS with model compounds, we can infer the elec-

(20) Bianconi, A.; Garcia, J.; Benfatto, M. In *Synchrotron Radiation in Chemistry and Biology I, Topics in Current Chemistry 145*; Springer-Verlag: Berlin, 1988; p 29.

(21) Stohr, J. *NEXAFS Spectroscopy*; Springer-Verlag: Berlin, 1992.

(22) Grunes, L. A.; Leapman, R. D.; Wilken, C. N.; Hoffmann, R.; Kunz, A. B. *Phys. Rev. B* **1982**, *25*, 7157.

(23) Aebe, P.; Erbudak, M.; Vanini, F.; Vvedensky, D. D.; Kostorz, G. *Phys. Rev. B* **1981**, *23*, 4369.

(24) van der Laan, G.; Westra, C.; Hass, C.; Swatzky, G. A. *Phys. Rev. B* **1981**, *23*, 4369.

(25) Muller, J. E.; Jepsen, O.; Wilkins, J. W. *Solid State Commun.* **1982**, *42*, 365.

(26) Bianconi, A.; Castellano, A. C.; De Santis, M.; Rudolf, P.; Lagarde, P.; Flank, A. M.; Marcelli, A. *Solid State Commun.* **1982**, *42*, 365.

(27) Meitzner, G.; Fischer, D. A.; Sinfelt, J. H. *Catal. Lett.* **1992**, *15*, 219.

(28) Sham, T. K. *Phys. Rev. B* **1985**, *13*, 1903.

(29) Chen, J.; Croft, M.; Xu, X.; Shaheen, S. A.; Lu, F. *Phys. Rev. B* **1992**, *46*, 15639.

(30) Bzowski, A.; Yiu, Y. M.; Sham, T. K. *Jpn. J. Appl. Phys. Suppl.* **1993**, Bzowski, A.; Sham, T. K.; Yiu, Y. M. *Phys. Rev. B* **1994**, *49*, 13776.

(31) Brown, M.; Peierls, R. E.; Stern, E. A. *Phys. Rev. B* **1977**, *15*, 738.

(32) Matheiss, L. M.; Dietz, R. E. *Phys. Rev. B* **1980**, *22*, 1665.

(33) Mansour, A. N.; Cook, Jr., J. W.; Sayers, D. E. *J. Phys. Chem.* **1984**, *88*, 2330.

(34) Tyson, C. C.; Bzowski, A.; Kristof, P.; Sammyreiken, R.; Kuhn, M.; Sham, T. K. *Phys. Rev. B* **1992**, *45*, 8811.

tronic structure of Cu on porous silicon. Since the Cu surface is oxidized in the ambient atmosphere to form a native oxide, we used Cu metal, CuO, and Cu₂O as model compounds in the comparative study reported herein.

Experimental Section

Porous silicon specimens were prepared as a circular thin film (~10 μm thick, 13 mm in diameter) on a 15 mm × 15 mm, 10 mil (0.25 mm) thick, p-type B-doped Si(100) wafer. The Si wafer was in contact with a circular Pt foil which was used as the electrical lead for the Si anode while a Pt wire was used as the counter electrode. Electrochemical etching of the Si wafer was carried out with an electrochemical cell in a 50–50 HF–ethanol solution at a constant current of 20 mA for 20 min. Samples prepared under these conditions exhibit a red-orange glow under UV and soft X-ray excitation and has a luminescence maximum⁹ at ~780 nm.

The reaction of Cu²⁺(aq) with PS was carried out at room temperature by dipping the as-prepared PS sample into a small beaker containing ~4 mL of an aqueous solution of CuSO₄ with a specific concentration (0.001, 0.01, or 0.1 M) for 5 min. Gas evolution was observed in all cases. After the reaction, optical microscopy revealed clearly the deposition of metallic particles on the PS surface from concentrated solutions. The luminescence intensity decreased considerably as the Cu concentration of the solution increased. These samples were stored in plastic vials at ambient atmosphere. All experiments were carried out in the ambient atmosphere. X-ray absorption measurements were made on month-old samples.

X-ray absorption experiments were made on the BL1A double-crystal monochromator (DXM) beamline at the 750 MeV UVSOR electron storage ring at the Institute for Molecular Science, Okazaki, Japan. UVSOR operates at a current of 200 mA at injection. Beryl crystals ($2d = 1.5965$ nm) were used as the monochromator providing photons with a resolution of <1 eV at the Cu L₃-edge (~930 eV). XANES were recorded in both the total electron yield (TEY) and the fluorescence yield (FLY) mode. Two methods (specimen current and channel-plate electron multiplier, CEM) were used in the TEY measurements. Both methods produce essentially the same spectrum with the CEM yielding three orders of magnitude better count rates, but the specimen current usually gives better signal-to-noise ratio despite the fact that the actual current measured is only of the order of 0.1 pA (Keithly current amplifier). The Cu L fluorescence X-rays were selected with a wide energy window and recorded with a gas proportional counter (GPC) filled with a mixture of argon and methane.^{35,36}

All XANES measurements were made at room temperature in a stainless steel vacuum chamber with a pressure of 10⁻⁸ Torr. Porous silicon specimens were mounted on a sample manipulator with four degrees of freedom ($x, y, z,$ and θ). The model compounds, Cu metal, and the oxides (CuO and Cu₂O) were in the form of a foil and powder thin films on a carbon tape, respectively. The Cu metal foil was cleaned by mechanical scraping in situ with a diamond file. The CEM and the GPC were mounted at 45° with respect to the incident beam at the opposite side of the chamber. Scattered light was minimized by rotating the sample with respect to the incident beam. We found that normal incidence gave a reasonable signal-to-noise for both detection modes and was used for most of the measurements. Energy calibration was done by observing the energy positions of the characteristic K-edge of the Na and Al components in the monochromator (beryl) crystal in the light curve obtained with a gold diode in the absence of the sample. Since the light curve in the Cu L-edge region is monotonic, the photon beam intensity (I_0) was monitored with the ring current. Both TEY and FLY measurements were

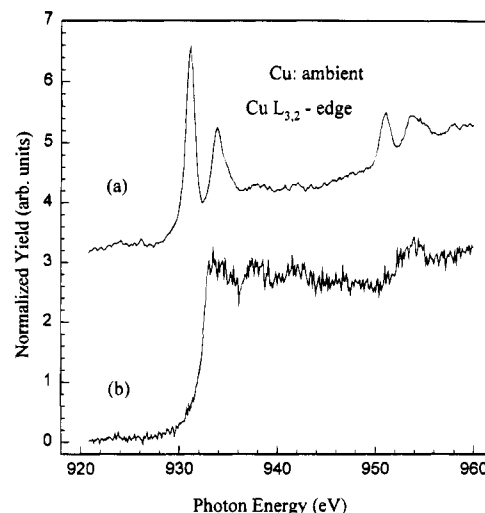


Figure 1. Cu L_{3,2} edge XANES of an ambient copper recorded in (a) TEY and (b) FLY mode.

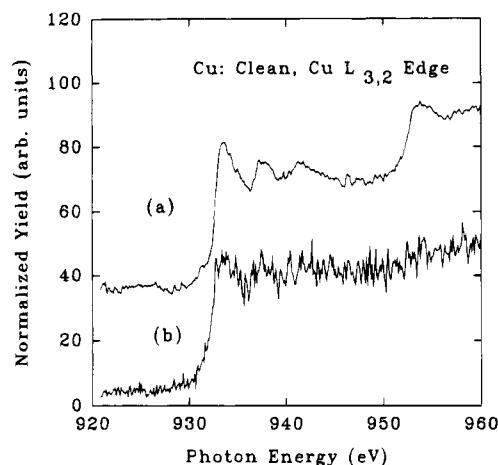


Figure 2. Cu L_{3,2} edge XANES of a clean copper (scraped in situ with a diamond file) recorded with (a) TEY and (b) FLY.

carried out simultaneously as the photon energy was scanned across the Cu L-edge. All the spectra displayed here are plotted as normalized yield (I_{yield}/I_0) vs photon energy.

Results

Figure 1 shows the Cu L_{3,2} edge XANES of an ambient Cu metal (~25 μm thick) recorded in both the TEY and FLY mode. The sharp peak at ~931 eV (L₃ edge) and ~951 eV (L₂ edge) of the TEY spectrum is assigned to surface CuO. The CuO peak in the FLY spectrum, however, is hardly noticeable, and the edge is dominated by Cu metal features. After cleaning (scraping in situ with a diamond file), the Cu metal exhibits identical spectra in both TEY and FLY measurements (Figure 2). A similar comparison of XANES of Cu(II) and Cu(I) oxide is seen in Figures 3 and 4, respectively. The spectra from both yields are nearly the same for CuO but there is a distinct difference in the case of Cu₂O whose TEY spectrum shows a sharp white line at ~931 eV followed by another peak at ~933 eV while the 931 eV peak is barely visible in the FLY spectrum.

The TEY spectra generally exhibit much better signal-to-noise ratio (S/N) than the FLY spectra. This is because TEY has virtually eliminated the "thickness effect" (self-absorption)³⁷ while the S/N ratio in the FLY

(35) Fischer, D. A.; Colbert, J.; Gland, J. L. *Rev. Sci. Instrum.* **1989**, *60*, 1596.

(36) Funabashi, M.; Ohta, T.; Yokoyama, T.; Kitajima, Y.; Kuroda, H. *Rev. Sci. Instrum.* **1989**, *60*, 2505.

(37) Stern, E. A.; Kim, K. *Phys. Rev. B* **1981**, *B23*, 3781.

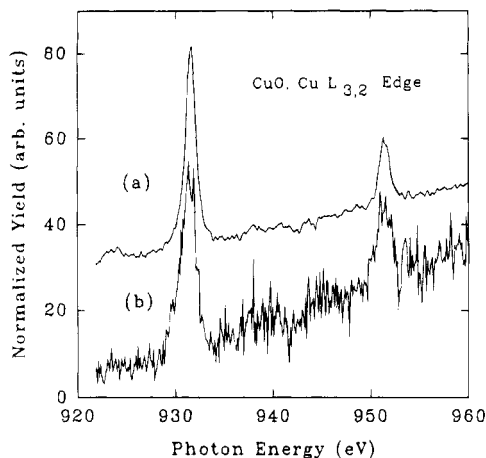


Figure 3. Cu $L_{3,2}$ edge of CuO: (a) TEY and (b) FLY.

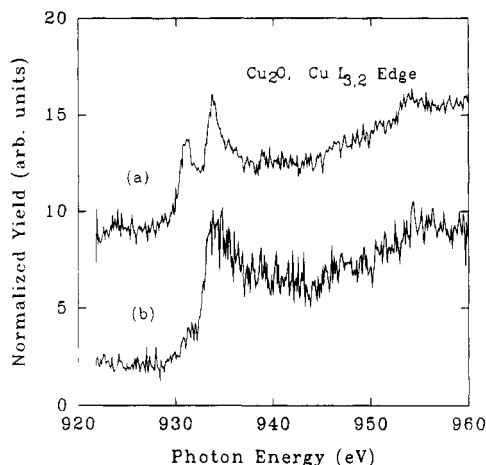


Figure 4. Cu $L_{3,2}$ edge of Cu_2O : (a) TEY and (b) FLY.

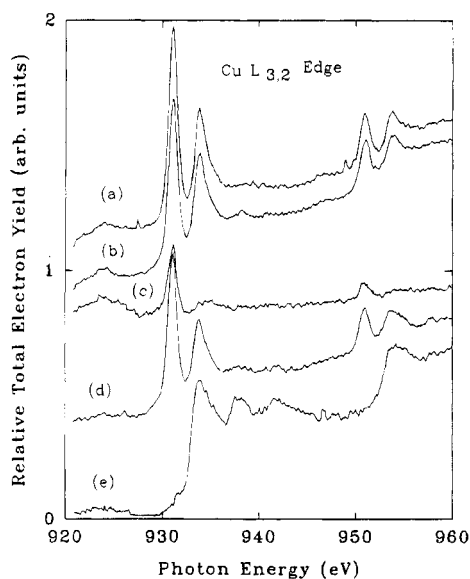


Figure 5. Comparison of $L_{3,2}$ edge XANES of Cu on porous silicon together with ambient and clean Cu recorded with TEY: (a) 0.1 M; (b) 0.01 M; (c) 0.001 M; (d) ambient Cu; (e) clean Cu.

mode is hampered by the low fluorescence yield and self-absorption, particularly in concentrated samples.³⁸

Figure 5 shows the TEY Cu $L_{2,3}$ -edge XANES of Cu/PS samples prepared from aqueous solutions of $CuSO_4$

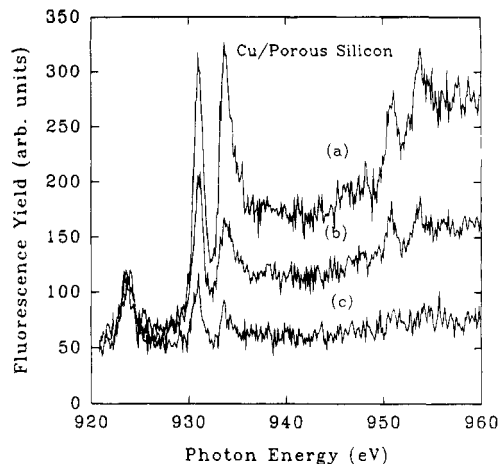


Figure 6. Comparison of Cu $L_{3,2}$ XANES of Cu/PS prepared from different $Cu^{2+}(aq)$ concentrations recorded with FLY: (a) 0.1 M, (b) 0.01 M, (c) 0.001 M.

with concentrations of 0.1, 0.01, and 0.001 M together with those of Cu metal under ambient conditions before and after cleaning. Except for the spectrum of the 0.001 M sample, all the Cu/PS spectra appear to be remarkably similar to those of the ambient Cu metal before cleaning, indicating the presence of Cu oxide on the surface. The XANES of the 0.001 M solution exhibits a negligible edge jump with a larger ratio of the intensity of the first to the second peak. Figure 6 shows the corresponding FLY XANES of the Cu/PS samples. They are similar to their TEY counterparts except that, relative to the intensity of the first peak at 931 eV, the absorption at ~ 933 eV (second peak) and the intensity of the edge jump are considerably higher and increase with increasing Cu concentration. The peak at 924 eV (below the edge) is seen in both TEY and FLY modes and is more intense in the latter, indicating that it is of bulk origin. We attribute it to the excitation of the Si substrate at the Si K-edge by second-order radiation (Si K-edge at $\sim 1840/2$ eV, Si oxide whiteline at $\sim 1847/2 = 923.5$ eV). The intensity of this 924 eV peak increases as the Cu^{2+} ion concentration (hence Cu coverage) decreases. The position of the L_3 edge resonances for the compounds of interest are compared in greater detail in Figure 7.

The size of the edge jump and the difference in absorption coefficient just above (~ 937 eV) and below (~ 925 eV) the edge also depend on the relative sample thickness in thin films. All the edge jumps exhibited in the Figures 5 and 6 are directly comparable since they have been normalized to the photon intensity. Parameters relevant to the discussion of the thickness of the Cu island of the Cu/PS samples are summarized in Table 1.

Discussion

Cu L-Edge Spectra of the Model Compounds: A Comparison of TEY and FLY XANES. Figures 1 and 2 show the $L_{3,2}$ edge XANES of an ambient Cu metal before and after in situ cleaning, respectively. The spike at ~ 931 eV (Figure 1) corresponds to the intense 2p to 3d transition of CuO (Figure 3) which is present on the surface of an ambient Cu foil. This peak is barely visible in the FLY detection which shows a more pronounced Cu metal XANES feature similar to that exhibited by a clean Cu in the total electron mode (Figure 2). Our Cu

(38) Jaklevic, J.; Kirby, J. A.; Klein, M. P.; Robertson, A. S.; Brown, G. S.; Eisenberger, P. *Solid State Commun.* **1977**, *23*, 679.

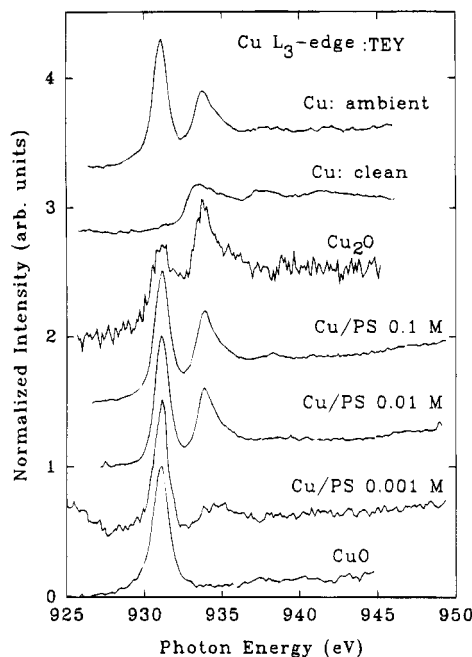


Figure 7. More detailed comparison of the Cu L₃ edge of Cu/PS samples (recorded with TEY) with those of model compounds; all spectra are normalized to the most intense peak (intensity = 1) except in clean Cu where the edge jump is normalized to that of the ambient Cu.

Table 1. Relevant Parameters for the Cu L₃ Edge XANES

sample	relative TEY edge jump ^a	peak positions (eV) ^b	assignment
Cu (ambient)	1.9	931.06	CuO
Cu (clean)	4.2	933.80	Cu metal
		937.5, 941.5	Cu metal
Cu/PS (0.1 M)	2.0 (120)	931.06	CuO
		933.80	Cu ₂ O, Cu metal
		938.08, 941.0	
Cu/PS (0.01 M)	1.9 (40)	931.06	CuO
		933.60	Cu ₂ O, Cu metal
		938.08, 941.0	Cu metal
Cu/PS (0.001 M)	~0.3 (15)	931.06	CuO
		934.5	Cu ₂ O, Cu metal
CuO	~0	931.06	CuO
Cu ₂ O	~0	931.06	CuO
		933.0	Cu ₂ O

^a Difference in absorption (normalized to photon flux) above (~937 eV) and below (~930 eV) the edge; values in parentheses are from the FLY; both are in arbitrary units. ^b Calibrated with respect to the whiteline of CuO at 931.06 eV.

XANES spectra are in good agreement with theoretical and experimental results reported in the literature.²²⁻²⁴ It is quite apparent from Figures 1 and 2 that the FLY is far more sensitive to the bulk signal than the total electron yield. The difference in sampling depth between the two techniques is crucial to our analysis of the XANES spectra for Cu on porous silicon. In general if a thick Cu film has been exposed to ambient atmosphere, the corresponding spectra should look like those of the ambient bulk Cu in both TEY and FLY detection. However if the Cu is thin (of the order of a monolayer), the surface oxide peak will be more intense than that of the Cu underneath in both detection schemes. As a result, the corresponding spectra will consist of a mixture of the spectra of the three model compounds with a dominant CuO feature in the XANES recorded with both detection schemes. This can be illustrated with the difference curve between the normalized FLY and the TEY XANES. The difference yields, semiquantitatively, the XANES of the surface component. Figure

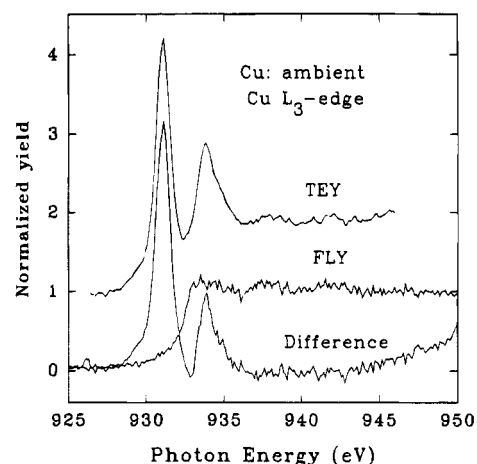


Figure 8. Subtraction of the normalized Cu L₃ edge FLY XANES of ambient Cu from its corresponding TEY XANES (both spectra are normalized to edge jump = 1); the TEY spectrum has been shifted upward by 1 unit for clarity. The difference curve corresponds to contributions from the surface sensitive components (Cu oxide).

8 shows the TEY and FLY XANES as well as the difference curve for the ambient Cu. It can be seen that the surface component is dominated by CuO (Figure 3) and it also exhibits a Cu₂O feature (Figure 4).

For CuO, both TEY and FLY XANES look similar except for the overall intensity and the signal-to-noise as expected. The whiteline corresponds to an excitation of a 2p electron to the unoccupied 3d states associated with a nominal 3d⁹ initial state and a 2pd¹⁰ (underline denotes a core-hole) final state of Cu(II). The d bands in Cu and Cu₂O are full, although there are some states of d character above the Fermi level, which accounts for the weaker whiteline seen at higher energies in Cu₂O^{24,39} and Cu metal²³ XANES. The Cu₂O XANES recorded with the two yields are different, however. The sharp feature at 931 eV in the TEY spectrum corresponds to the whiteline position of CuO, and it diminishes in the FLY spectrum indicating that it is a surface component. Thus it is suggested that Cu₂O stored in the ambient has a surface Cu(II) oxide component. Spectra of these model compounds are used here to assist the assignment of the Cu/PS spectra. A more detailed comparative study of the model compounds, as revealed by simultaneous measurements with these techniques, will be reported elsewhere.

Cu L-Edge XANES of Cu on Porous Silicon and Their Implications. The Cu L-edge XANES of Cu deposited on porous silicon from solution can now be interpreted qualitatively in terms of the spectra of the model compounds. From Figures 4 and 5, we see that the TEY spectra for the samples prepared from 0.1 and 0.01 M CuSO₄ solutions are quite similar to each other and to the corresponding TEY spectrum of ambient Cu metal while the FLY spectra are much closer to the TEY spectra than in the case of an ambient Cu metal where TEY and FLY XANES exhibit dominant Cu oxide and Cu metal features, respectively. (For practical purposes, a 25 μm thick Cu film is infinitely thick for both detection techniques used here.) In either case, we can assign the first sharp peak to the whiteline position of CuO and the second to that of Cu₂O and Cu contributions (see Figures 1-4 and Table 1). This result

indicates that a significant fraction of the Cu in Cu/PS samples is on the surface and is oxidized to Cu oxide as in the case of an ambient Cu metal. The presence of unoxidized Cu is deduced from a comparison of the FLY and TEY spectra (see below), although the signal from the unoxidized Cu underneath, unlike bulk metal, is not clearly visible in the FLY spectra, especially at low CuSO₄ concentration (0.001 M) and becomes only a little more noticeable for higher concentrations (0.1 and 0.01 M, Figures 5 and 6).

The relative thickness of the oxide and the unoxidized Cu in the Cu/PS specimens can be estimated semiquantitatively from the edge jump and the intensity of the whiteline relative to the edge jump (Table 1). Let us consider the TEY XANES for the moment, the size of the edge jump is related to the thickness of the Cu film within the thin film limit in which the signal is sensitive to the near-surface region of the specimen since the kinetic energy for the electrons (photo, Auger, and secondary) responsible for the TEY is low, leading to short escape depths.

At the Cu L-edge photon energy the infinite thickness limit for TEY can be reached with tens of monolayers. Such a limit is governed by the electron escape depth. For example, if the electron escape depth is ~ 1 nm, typical for electrons produced by Cu L-edge absorption, the thickness required to produce a 90% bulklike signal is only ~ 10 layers (2.5 nm) of Cu. Furthermore, if Cu is covered by Cu oxide, the overall Cu edge jump will be reduced by 50% by an oxide layer with a thickness of ~ 3 –4 monolayer (0.7–1 nm). This is because the XANES of pure Cu has a sizable edge jump, while CuO has a negligible edge jump; therefore, the unoxidized Cu underneath is primarily responsible for the edge jump intensity in Cu/PS samples. This property of Cu and CuO as model compounds can be used to monitor the relative contribution of Cu and Cu oxide to the observed edge jump (Table 1).

From Table 1, we see that there is a 50% reduction in the relative edge jump between clean and ambient Cu before cleaning in the TEY measurement. This difference can be attributed to the presence of several monolayers of a native oxide. The 0.1 and 0.01 M Cu/PS exhibit edge jumps nearly identical to that of the ambient Cu, indicating that they have very similar structure in the near surface region that can be detected by TEY. The corresponding FLY edge jump samples much further into the solid than the TEY and it shows, at least qualitatively, that there is a substantial difference between the FLY spectra of Cu/PS and that of ambient Cu although they exhibit the same TEY features and there is a noticeable increase in the Cu coverage underneath the surface oxide as the Cu ion concentration increases (Figure 6 and Table 1). This indicates that the Cu on PS is very thin (\sim monolayer); therefore, even in the most concentrated case, the thickness has yet to reach the thick coverage limit (100 nm) that can be sampled by FLY. The relative edge jump exhibited by the FLY spectra shown in Table 1 varies linearly with the Cu²⁺(aq) concentration. The intensity of the substrate signal at 924 eV also supports this trend.

The presence of Cu underneath the CuO film in Cu/PS can also be seen more clearly when the Cu oxide contribution to the Cu/PS spectrum is removed by subtracting the TEY XANES (dominated by the surface

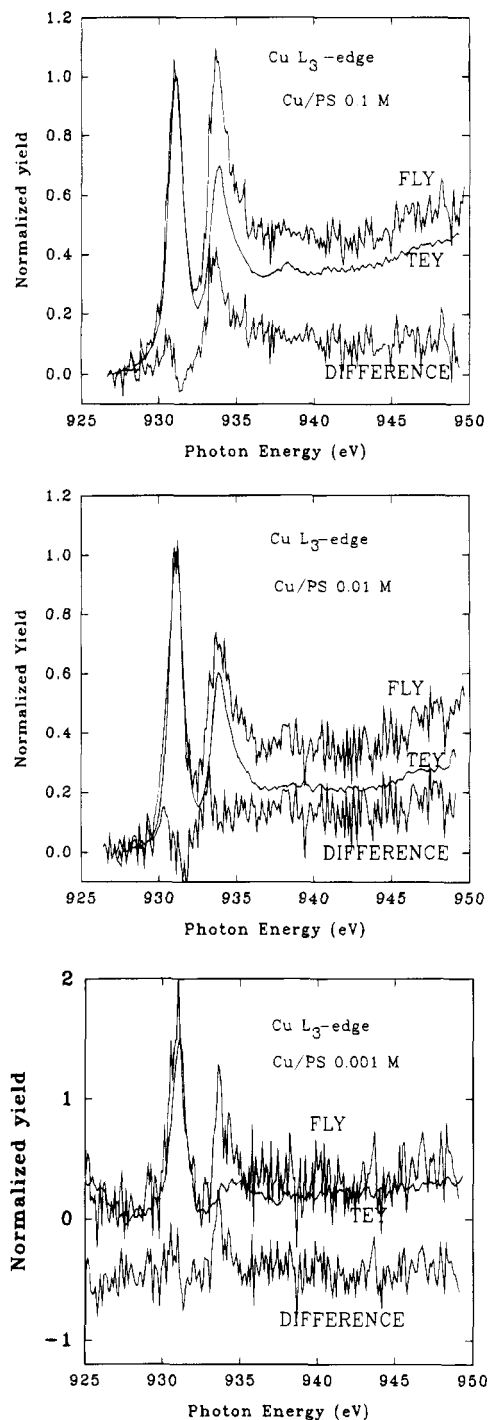
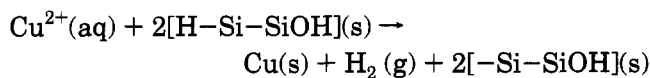


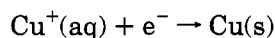
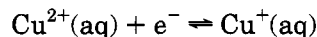
Figure 9. Comparison of TEY and FLY XANES for Cu/PS samples; spectra are normalized to the first sharp peak; the difference curve is also shown: (a, top) 0.1 M; (b, middle) 0.01 M; (c, bottom) 0.001 M.

component) from the FLY spectrum (bulk sensitive). This is shown for in Figure 9, where the difference curve clearly exhibits an edge jump corresponding to the unoxidized Cu underneath for at least the 0.1 and 0.01 M sample.

The above observation may be understood semiquantitatively on the basis of the stoichiometry of the oxidation–reduction reaction at the liquid–solid interface. The reaction must involve the reduction of Cu²⁺ by Si surface sites most likely containing adjacent Si–H and Si–OH. The presence of these sites have been confirmed by infrared spectroscopy. Although the details of the chemistry have yet to be worked out, it is probable that the following is the net reaction:



It has been known for many years^{40,41} that reduction of Cu^{2+} in acidic solutions is a two-step process:



with the slow $\text{Cu}^{2+}-\text{Cu}^+$ exchange the rate-limiting step. In solutions of copper salts with no added acid, there is a substantial content⁴² of $\text{Cu}_2(\text{OH})_2^{2+}$ arising from hydrolysis of Cu^{2+} . While the electrode kinetics of reduction and deposition of copper from neutral solution remains obscure, Fletcher et al.⁴³ have suggested that oxidation of copper in alkaline solution proceeds via dissolution of $\text{Cu}(\text{I})$ hydroxy complexes to form eventually a layer of Cu_2O , and Ambrose et al.⁴⁴ have produced some evidence that reduction to Cu_2O occurs from complexes such as $\text{Cu}(\text{OH})_4^{2-}$. Here, in the slightly acidic solutions resulting from hydrolysis, $\text{Cu}(\text{OH})_2$ can precipitate on the substrate and convert to CuO on drying, while Cu_2O can form through partial reduction of $\text{Cu}_2(\text{OH})_2^{2+}$.

The Cu film consists of Cu islands, and is formed by diffusion-limited growth of Cu atoms following reduction and nucleation; a similar phenomenon has been observed for Pd deposited reductively on porous silicon except that in the case of Pd the surface is resistant to oxidation. To a first approximation, the volume (4 mL) of CuSO_4 solution used in the experiment provides $\sim 2.4 \times 10^{21}$ Cu atoms for a concentration of 1 M. This conversion factor, when multiplied by the actual concentration and divided by an estimated effective surface area of $\sim 260 \text{ cm}^2$ of our porous silicon sample surface,⁴⁵ amounts to a coverage of the order of hundreds of monolayer, tens of monolayers, and monolayers of Cu for 100% conversion from $\text{Cu}^{2+}(\text{aq})$ to Cu for solutions of concentrations 0.1, 0.01, and 0.001 M, respectively. It is expected that the oxidation-reduction process reaches completion when all the active surface sites are consumed. Should this be the case, the number of Cu atoms deposited would be limited by the number of active sites as well as Cu^{2+} ions available and would lead to a maximum coverage of the order of a monolayer of Cu on the internal PS surface to as much as $1 \mu\text{m}$ deep, although surface diffusion will take place to form two-

or three-dimensional islands on the PS surface; the surface Cu inevitably becomes oxidized when the sample is exposed to the ambient atmosphere.

Returning to Figures 6 and 7, we see that the 0.001 M sample exhibits an oxide-like signal indicating that most of the Cu deposited on PS is oxidized to CuO (Figure 9) while for the 0.1 and 0.01 M samples some unoxidized Cu remains underneath the surface oxide. This is consistent with the stoichiometry of the reaction as well as the ion concentration. These observations indicate that for the same batch of PS samples prepared under identical conditions (same surface area), and in the absence of countervailing kinetic arguments, the reaction depends on the initial Cu ion concentration: in the case of the 0.1 and 0.01 M solutions Cu(II) ions are in excess and comparable to the number of active surface sites, while for the 0.001 M solution the number of surface Cu atoms is clearly smaller than the number of active sites as indicated in Figures 5 and 6 by the relative intensity of adsorbates and substrate.

Conclusion

In this paper we have shown, using high-resolution X-ray absorption spectroscopy, that reductive deposition of Cu metal on porous silicon takes place at the liquid-solid interface and depends on the number of active surface sites and the concentration of Cu ion. It is interesting to note that there is a remarkable similarity between this system and the Ru-Cu bimetallic catalysts.⁴⁶⁻⁴⁹ The ready oxidation of Cu on exposure to the ambient atmosphere is characteristic of both systems. Although the details of the chemistry and the kinetics of Cu island formation still need to be worked out, there is no doubt that Cu can be dispersed on the inner surface of porous silicon reductively from aqueous solution under controlled conditions. This reducing property of porous silicon makes it a desirable reducing agent for modest oxidation reduction reactions and has implications for the design and fabrication of noble metal and bimetallic catalysts⁵⁰ on silica supports. Research along these directions is presently in progress in our laboratories.

Acknowledgment. T.K.S. wishes to acknowledge the Japan Society for the Promotion of Science (JSPS) for a fellowship at UVSOR, Institute for Molecular Science and the hospitality of the staff of UVSOR where part of this work was carried out. Research at the University of Western Ontario is supported by Natural Science and Engineering Research Council (NSERC) of Canada and the Ontario Centre for Materials Research (OCMR). SRC is supported by the US National Science Foundation (NSF).

(40) Bockris, J. O'M.; Mattson, E. *Faraday Soc., Trans.* **1959**, *55*, 1586.

(41) Brown, O. R.; Thirsk, H. R. *Electrochim. Acta* **1965**, *10*, 383.

(42) Baes, C. F.; Mesmer, R. E. *The Hydrolysis of Cations*; Wiley-Interscience: New York, 1976; Section 12.1.2.

(43) Fletcher, S.; Barradas, R. G.; Porter, J. D. *J. Electrochem. Soc.* **1978**, *125*, 1960.

(44) Ambrose, J.; Barradas, R. G.; Shoesmith, D. W. *Electroanal. Chem. Interfacial Electrochem.* **1973**, *47*, 47.

(45) A lower bound estimate using a surface area of $\sim 1 \text{ cm}^2$ and assuming that the sample has an internal surface area of $200 \text{ m}^2/\text{cm}^3$ and an effective thickness of $\sim 1 \mu\text{m}$. The effective thickness was estimated from SEM measurements of which a Cu-riched layer of $\sim 1 \mu\text{m}$ was clearly visible from SEM micrograph of the cross section of a fractured sample taken after a typical PS sample had been immersed in a 0.001 M CuSO_4 solution for 5 min.

(46) Sinfelt, J. H.; Lam, Y. L.; Cusumano, J. A.; Barnett, A. E. *J. Catal.* **1976**, *42*, 227.

(47) Sinfelt, J. H.; Via, G. H.; Lytle, F. W. *J. Chem. Phys.* **1980**, *72*, 4832.

(48) Sham, T. K.; Ohta, T.; Yokoyama, T.; Takata, Y.; Kitajima, Y.; Funabashi, M.; Kuroda, H. *J. Chem. Phys.* **1991**, *95*, 8725.

(49) Sham, T. K.; Liu, Z.-F.; Tan, K. H. *J. Chem. Phys.* **1991**, *94*, 6250.

(50) Sinfelt, J. H. *Bimetallic Catalysts: Discoveries, Concepts, and Applications*; John Wiley & Sons: New York, 1979.